OPO OPHTHALMIC & PHYSIOLOGICAL OPTICS
THE JOURNAL OF THE COLLEGE OF OPTOMETRISTS

Ophthalmic and Physiological Optics ISSN 0275-5408

Optical and imaging properties of a novel multi-segment spectacle lens designed to slow myopia progression

Matt Jaskulski, Neeraj K Singh, Arthur Bradley and Pete S Kollbaum

Indiana University School of Optometry, Bloomington, IN, USA

Citation information: Jaskulski M, Singh NK, Bradley A, & Kollbaum PS. Optical and imaging properties of a novel multi-segment spectacle lens designed to slow myopia progression. *Ophthalmic Physiol Opt*2020. https://doi.org/10.1111/opo.12725

Keywords: DIMS, image quality, myopia control, optical aberration, spectacles

Correspondence: Matt Jaskulski
E-mail address: mateusz.jaskulski@gmail.com

Received: 16 May 2020; Accepted: 7 July 2020

Abstract

Purpose: High sampling density optical metrology combined with pupil- and image-plane numerical analyses were applied to evaluate a novel spectacle lens containing multiple small zones designed to slow myopia progression.
Methods: High-resolution aberrometry (ClearWave, www.lumetrics.com) was used to sample wavefront slopes of a novel spectacle lens, Defocus Incorporated Multiple Segments (DIMS) (www.hoya.com), incorporating many small, positive-powered lenslets in its periphery. Using wavefront slope and error maps, custom MATLAB software ('Indiana Wavefront Analyzer') was used to compute image-plane point-spread functions (PSF), modulation transfer functions (MTF), simulated images and power distributions created by the dual-focus optic for different pupil sizes and target vergences.
Results: Outside of a central 10 mm zone containing single distance optical power, a hexagonal array of small 1 mm lenslets with nearest-neighbour separations of 0.5 mm were distributed over the lens periphery. Sagittal and curvature-based measures of optical power imperfectly captured the consistent +3.50 D add produced by the lenslets. Image plane simulations revealed multiple PSFs and poor image quality at the lenslet focal plane. Blur at the distance optic focal plane was consistent with a combination of diffraction blur from the distance optic and the approximately +3.50 D of defocus from the 1 mm diameter near optic zones.
Conclusion: Converging the defocused beams generated by the multiple small (1 mm diameter) lenslets to a blurred image at the distance focal plane produced a blur magnitude determined by the small lenslet diameter and not the overall pupil diameter. The distance optic located in between the near-add lenslets determines the limits of the optical quality achievable by the lens. When compared to the optics of a traditional concentric-zone dual-focus contact lens, the optics of the DIMS lens generates higher-contrast images at low spatial frequencies (<7 cycles per degree), but lower-contrast at high spatial frequencies.

1. Introduction

Prevalence of myopia has been increasing globally,[1] and in select East-Asian populations can exceed 95%.[2,3] High levels of myopia are associated with significantly elevated risk of developing retinal complications, potentially leading to severe visual impairments in later life.[4] Therapeutic interventions have been developed that include environmental control,[5] pharmaceutical drops,[6] optical manipulations that introduce multifocal optics[7-9] or contrast-attenuation filters.[10]

A novel dual-focus (bifocal) spectacle lens, which includes discrete, positive-power lenslets on its surface[11] has been employed as a myopia control device,[12] showing a certain degree of success. We have examined the imaging properties of this Defocus Incorporated Multiple Segments

(DIMS) lens (www.hoya.com), the design of which is unique in the field of ophthalmic dual-focus lenses, which are generally included in contact lenses[13,14] or intraocular lenses.[15,16] Precursor dual-focus lenses designed for presbyopes and pseudophakic eyes distribute distance and near optical corrections into different geographic zones across the lens and hence across the eye's pupil,[17] and work by creating a high-quality image when either the distance or near optic is focused on the retina.[14-18] To create a near image, the optics of each near zone must create a single focused image (*Figure 1a*). The new DIMS spectacle lens employs a zonal structure containing small, circular (≅1 mm diameter) lenslets, each containing add power, but images from each individual lenslet do not converge to create a single image in the focal plane corresponding to the add power (*Figure 1b*), but rather multiple separate images.[11] The present investigation examined the optical and imaging ramifications of this novel lens design.

2. Methods

A high-resolution single-pass Shack-Hartmann aberrometer with a 540 nm light source (ClearWave, www.lumetrics.com) was used to sample wavefront slopes every 104 microns[19] across a 10 mm aperture. Local integration methods were used to compute wavefront error maps of the pupil,[20] which were exported for analysis with custom imaging software (Indiana Wavefront Analyzer, IWA) running in MATLAB™ (https://www.mathworks.com/products/matlab.html). Wavefront slopes across a 9.3 mm measurement aperture were measured in one central, and two peripheral regions of a sample DIMS lens with distance correction of −0.50 D (*Figure 2*).

Wavefront error maps were corrected for astigmatism and prism, and local horizontal and vertical wavefront slopes were obtained from the wavefront by means of numerical differentiation. Sagittal power at each point in the pupil was computed by dividing radial wavefront slopes by radial distance from the pupil centre $(dW/dr)/r$.[21] Power was additionally calculated using the local curvature of the wavefront $(d^2W_x/dx^2 + d^2W_y/dy^2)/2$.[22] Fourier Transforms of the pupil functions were used to compute point-spread functions (PSFs) and modulation transfer functions (MTFs) in the image plane. Simulated images were computed by convolution.[23]

3. Results

Both visual inspection and wavefront metrology reveal a central lenslet-free region of approximately 10 mm, surrounded by an annular region containing lenslets 1 mm in diameter arranged in a triangular array with nearest neighbour centre-to-centre distance of approximately 1.5 mm giving a coverage factor of approximately 40% (*Figure 2*).

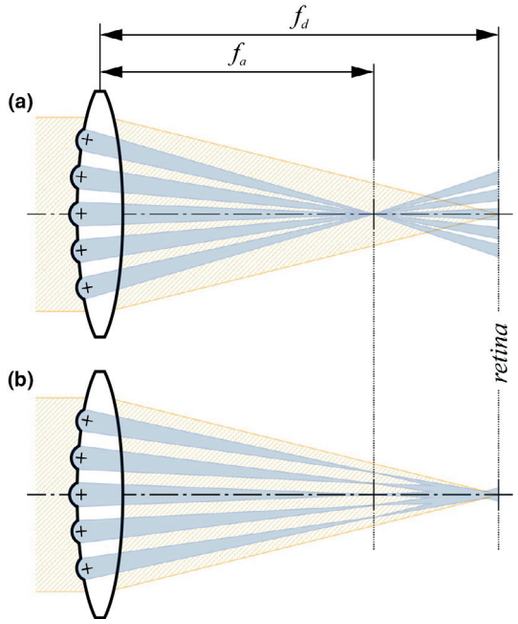

Figure 1. Schematic ray tracing of zonal bifocal lenses showing destinies of individual ray bundles passing through the near add zones (blue rays) and the distance base optic (yellow rays) being focused, respectively, at f_a (add) and f_d (distance). Lens design (a) shows a traditional zonal bifocal design, with a single focus at each focal plane, and (b) shows the novel focusing pattern of add zones that converge to a single blur pattern at the distance focal plane, but create multiple individual foci at the near focal plane.

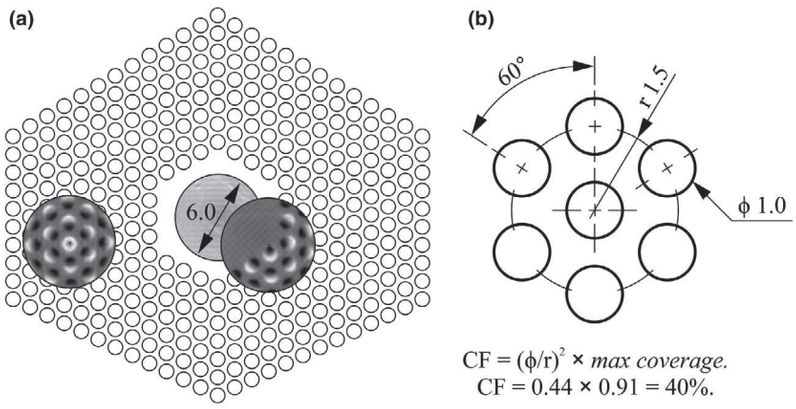

Figure 2. Geometry of the DIMS spectacle lens. (a) 1 mm diameter circular lenslets are arranged in a hexagonal pattern spaced along the primary meridian by centre-centre distances of 1.5 mm resulting in nearest neighbour separations of 0.50 mm (b). Three large circles in *Figure 2a* represent three 6.0 mm diameter locations on the DIMS lens that were sampled for optical analyses. Each 6.0 mm sample includes the corresponding radial wavefront slope maps sampled using a single-pass Shack-Hartmann aberrometer. CF stands for coverage factor, which is equal to the square of the ratio between the lenslet diameter and lenslet separation, multiplied by the maximum coverage factor (0.91) when said ratio is equal to 1.

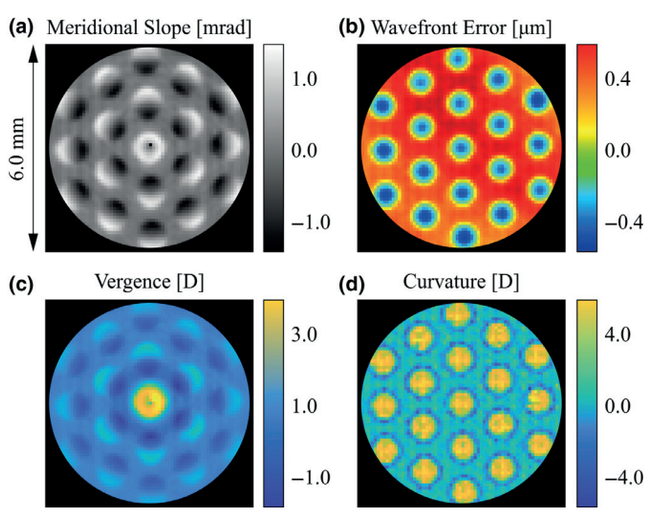

Figure 3. Wavefront slope (a), Wavefront error (b), Sagittal Power (c) and Curvature Power (d) maps from the 6.0 mm sample located in the DIMS lens peripheral region.

Example radial wavefront slope (mrad), wavefront error (microns), sagittal power (dioptres) and local curvature power (dioptres) are shown over a 6.0 mm analysis pupil centred in a region fully populated with the 1 mm diameter lenslets from a DIMS lens with a distance power of −0.50 D and power in the add zones of +3.00 D (*Figure 3a-d*). The wavefront slope changes across each 1 mm diameter lenslet are quite uniform (*Figure 3a*) with an edge-to-edge slope difference of 1.5 mrad, consistent with the expected +3.00 D of positive power in each lenslet.

When utilising the aforementioned radial 'slope/r' calculation to obtain sagittal power, only the central lenslet power is correctly reported (+3.00 D, *Figure 3c*), while the base power of −0.50 D is observed across the full measurement aperture. At the same time, powers of lenslets not centred on the measurement pupil are all underreported, which is anticipated because whereas the radial wavefront slopes within each lenslet are almost identical (*Figure 3a*), the distance from centre *r* increases, resulting in the decrease in calculated power. When power is calculated by the local curvature of the wavefront (obtained by calculating the second derivative of the wavefront), each lenslet power is correctly reported (*Figure 3d*). However, this method evaluates differences in local slopes, and reports

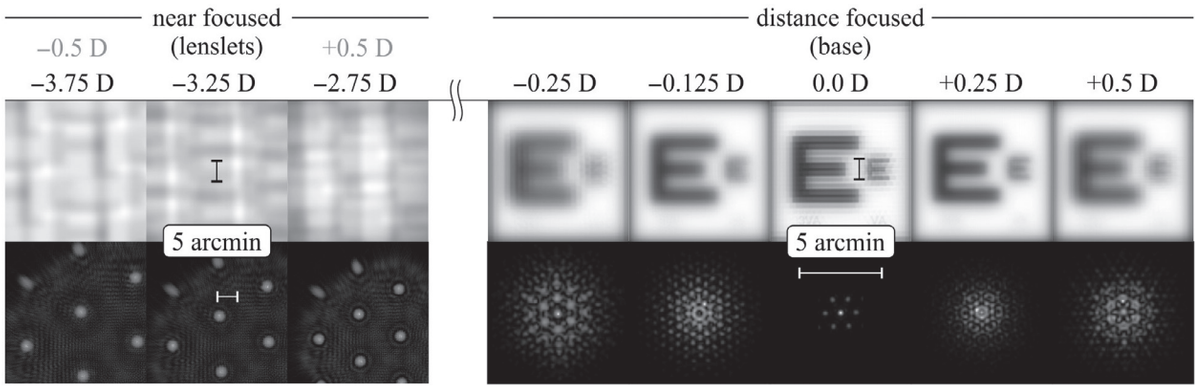

Figure 4. Point Spread Functions (PSFs) and simulated images of high contrast letter E targets (20/60 and 20/20) computed for a range of target vergences (values indicated above each panel) centred on the TVs required to focus the near (left) and distance (right) optics. Pupil diameter = 6.0 mm, sampled aperture fully within the peripheral lenslet region of the DIMS spectacle lens (see *Figure 2a*).

anomalous powers at the margins of each zone (note the dark blue ring indicating highly negative powers at the borders of the lenslets). The −6.00 D ring observed in the curvature power maps is not present in the optical design, and is an artifact created because sampled rays just inside and just outside of each lenslet will diverge relative to each other. The above analysis reveals the challenges of accurately reporting power of lenslets in the DIMS lens.

Image plane calculations do not require a power determination, but instead employ a Fourier Transform of the pupil function (wavefront error map across the pupil,[24] *Figure 3b*). *Figure 4* shows sample PSFs and simulated images of 20/20 and 20/60 high contrast letter E's for a 6.0 mm pupil sampled from within the area of the DIMS lens completely covered by lenslets, while *Figure 5* shows the same for a pupil that is approximately 50% covered by lenslets.

PSFs at and near to the distance focus (*Figures 4 and 5*, right panels) are small with sufficient image quality at the focal plane to image a 20/20 character. By contrast, the multiple individual PSFs superimposed on the large blur from the distance optic seen at and near the near lenslet focal plane (*Figures 4 and 5*, left panels) lead to low contrast and multiple repeated images. As the image plane moves farther from the distance optical focal plane, the image quality generated by the large aperture distance optic decreases rapidly, and the distance optic blur pattern expands in diameter becoming large at the near optic focal plane (*Figures 4 and 5*, left panels).

Blur associated with the 1 mm diameter lenslets remains dominated by diffraction over the 1.00 D range of defocus (*Figures 4 and 5*, left panels), and the array of lenslets within the measurement aperture generate an array of spatially separated PSFs as predicted from the schematic in *Figure 1b*. The simulated retinal images around the near focal plane of the lenslets reveal multiple repeated images, each with reduced contrast because each lenslet contributes

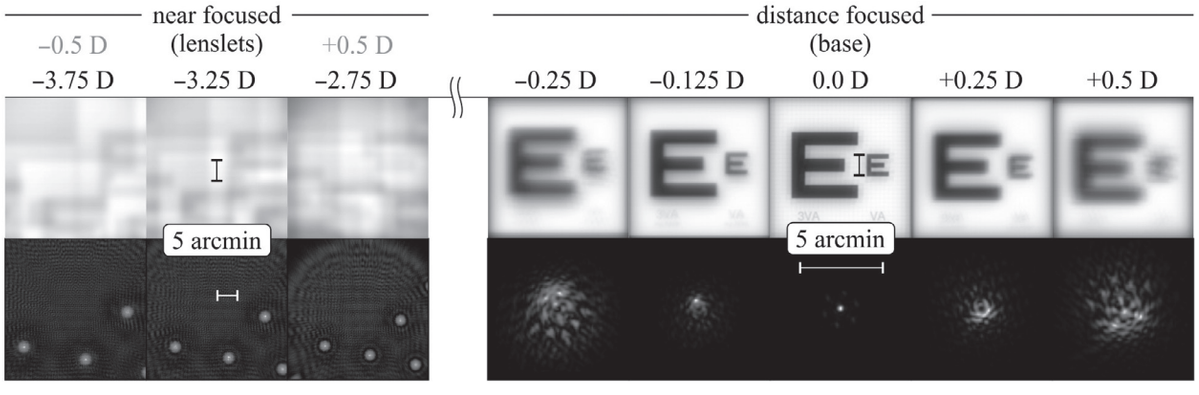

Figure 5. Point Spread Functions (PSFs) and simulated images of high contrast letter E targets (20/20 and 20/60) computed for a range of target vergences (values inset in each panel) with zero being the target vergence that focused either the distance optic (right). Pupil diameter = 6.0 mm for an aperture that was partially (~50%) covered by the lenslet region of the DIMS spectacle lens (see *Figure 2a*).

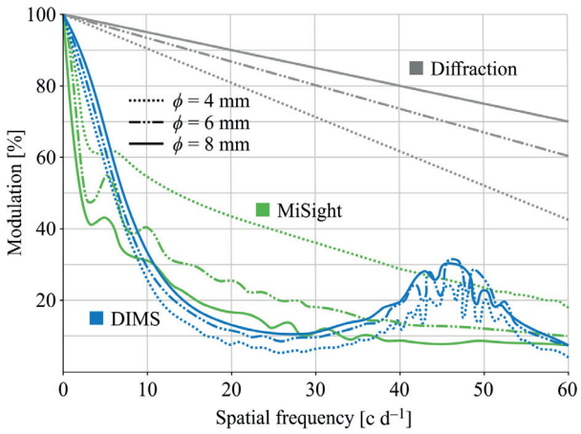

Figure 6. MTFs computed when the distance optic is focused for both the DIMS multi-zone spectacle lens (blue lines) and the MiSight multi-zone contact lens (green lines). For each lens, MTFs were computed for pupil diameters of 4.0 mm, 6.0 mm and 8.0 mm. Full aperture diffraction limited MTFs are shown for comparison (grey lines). The comparison MiSight lens has a 'centre-distance' optic surrounded by annular zones containing +2.00 D add power (zones 2 and 4), and a second distance optic (zone 3), with outer diameters of approximately 3.3 mm, 4.9 mm, 7.1 mm and 8.9 mm, respectively.[25]

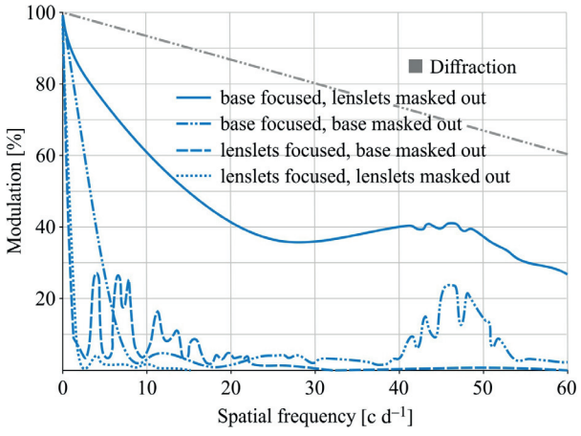

Figure 7. MTFs for the isolated distance and near components of a DIMS lens. The focused isolated distance (base) and near (lenslet) optics are represented by solid and dashed blue lines, respectively and the corresponding defocused optics by dotted and dot-dash lines, respectively.

only $(1/6)^2$ of the light in the image. Image quality at the distance optic focal plane is approximately diffraction limited for an analysis pupil centred on the DIMS centre lacking any lenslets (data not shown), and when the lenslets populate about 50% of the measurement pupil (*Figure 5*) the distance focal plane image quality is superior to that achieved when the full pupil is populated with lenslets (*Figure 4*).

Quantitative analysis of the image quality generated at the distance optic focal plane of the DIMS lens region fully populated by lenslets was performed using MTFs (*Figure 6*). Diffraction blur for a single focal power optic (grey lines) changed significantly over the 4-8 mm pupil diameters. However, the real MTFs (blue lines) remained similar for each pupil size, revealing a significant drop in image modulation between zero and 20 cycles per degree (c d^{-1}) and an increase in image modulation around 45 c d^{-1}. This pupil size independence is quite different from that seen with more traditional zonal bifocal designs (e.g. *Figure 6* green lines).

Image contrast at each of the focal planes of a traditional zonal bifocal lens is determined jointly by the significant diffraction blur created by the segmented and potentially narrow annular apertures, and the amount of defocused light contributed by the out-of-focus optics.[14] In the case where the apertures creating the focused image are small (e.g. narrow annular apertures in a concentric zonal bifocal lens), the focused MTF includes a drop at low spatial frequencies due to diffraction at the small sub-aperture size (width), but the total bandwidth is determined by the sum of local sub apertures (e.g. total diameter of the annular zone).[14] Since in the DIMS design the gaps between nearest-neighbour lenslets containing the distance optic are only 0.5 mm (*Figure 2b*), a drop in the MTF paralleling that created by a 0.5 mm diameter pupil (dropping to zero at about 15 c d^{-1}) contributes to the reduced modulation at low spatial frequencies at the distance optic focal plane (*Figure 6*). The increase in image modulation seen at higher spatial frequencies mirrors the effect seen in the diffraction-limited MTFs of a thin, annular-aperture lenses.[14] Also, the approximately +3.50 D defocus created by the multiple lenslets generates a localised defocused image at the distance focal plane (*Figure 1b*). Using Smith's equation to predict blur circle size (B = PD) a blur of 0.2 degrees is predicted, which will create an MTF that drops to zero at about 6 c d^{-1}.[26] Therefore, diffraction from the focused distance optic and defocus of the near optic are both contributing to the drop in the MTFs over the range of approximately 0-15 c d^{-1}.

MTFs reveal higher contrast generated with small pupils when imaging through the centre of a traditional, zonal, dual-focus lens (*Figure 6*, green lines, this model contains a 3.3 mm diameter distance optic centre zone). With pupil sizes large enough to include both the distance and near optics of the traditional zonal bifocal lens, the distance optic's focal-plane MTFs are attenuated by the amount of defocused light created by the near optic. When comparing these two lens designs, one can see that the DIMS design produces higher modulation below 5-8 c d^{-1}, but lower image modulation above 10 c d^{-1}. In terms of image formation, this result would translate to images with higher

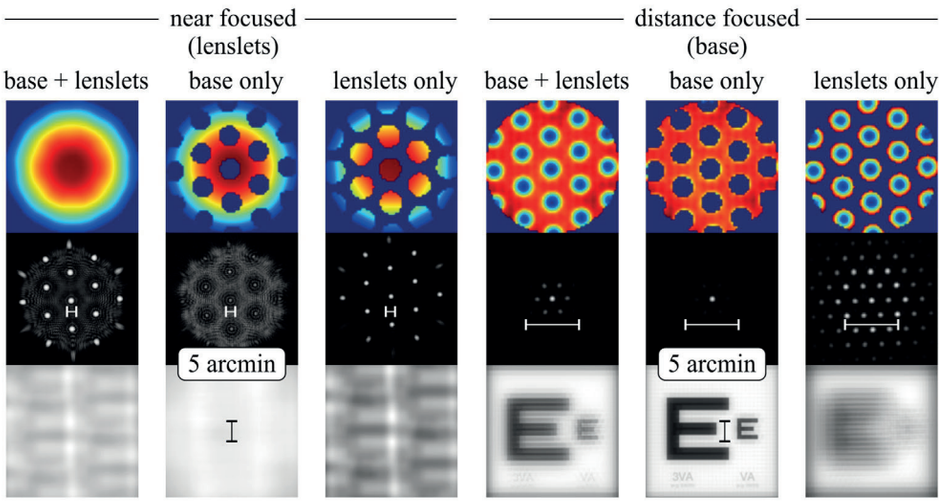

Figure 8. Wavefronts and images generated by the combined distance and near optics, and each optic isolated, were computed at the near optic focal plane (left three panels) and distance optic focal plane (right three panels). The top panels show the wavefront error maps, and middle and bottom panels show images of PSFs and 20/20 together with 20/60 letter E's, respectively. At the near focal plane, the PSFs generated by the near optic are a series of spatially-separated diffraction-limited points, whereas the out-of-focus distance optic generates a familiar large blur circle, but with areas absent due to the masking out of the lenslets. The out-of-focus but converged near optic lenslets create a series of localised diffraction limited PSFs in their focal plane (see schematic in *Figure 1b*).

contrast, but more blur generated by the DIMS lens compared to the traditional zonal bifocal design, which has much greater blur created by the near add zone, but a higher quality focused image generated by the distance optic.

The image quality at both distance- and near-image planes results from the combined impact of an array of near add power lenslets and a distance optic that exists at all locations other than the lenslets. Therefore, we examined the optical quality provided by each contributing optic (*Figure 7*). For example, the MTFs generated by the focused distance optic aperture drop below 40% at 25 c d^{-1}, but increase to >40% at 45 c d^{-1}. The defocused lenslet images (which approximately superimpose at the distance focal plane, *Figure 1b*) produce an MTF which drops to zero at about 9 c d^{-1}, as predicted from simple geometrical optics. The resulting MTF (*Figure 6*) is therefore a 60/40 weighted combination of the two-component optical MTFs seen in *Figure 7*. At the near focal plane, the resultant image is a combination of that produced by the 3.50 D defocused distance optic and the focused near optic generating multiple images. Both component MTFs are shown in *Figure 7*, neither yielding high image quality.

The wavefronts used to generate the images for each component optic are shown in the upper panels of *Figure 8*, and the resulting images of a point source and small letter E's are shown in the middle and bottom panels, respectively. The three left panels in *Figure 8*, labelled 'near focused', were computed for the near optic (lenslets) focal plane, whereas the three right panels, labelled 'distance focused', were computed for the distance (base optic) focal plane. The wavefront error map of the distance optic at its own focal plane is quite flat and dominated by spherical aberration ('distance focused, base only' panel in *Figure 8*), whereas the wavefronts of each small lenslet optic are highly curved due to the 3.5 D of defocus ('distance focused, lenslets only' panel in *Figure 8*). On the other hand, at the near optic focal plane there is no local curvature in the wavefronts of each lenslet (compare the 'lenslets only' panels for both 'near focused' and 'distance focused' conditions). The significant negative curvature in the base optic wavefront is observed at the near optic focal plane in the wavefronts of both the distance and near optics (see the 'near focused, base only' and 'near focused, lenslets only' panels). If the DIMS was a traditional bifocal lens, the wavefront error maps within each lenslet region would be flat at their focal plane, but the unique design of the DIMS lens retains the wavefront slopes expected from the out-of-focus distance optic across the pupil. Each lenslet introduces wavefront curvature but retains the overall wavefront slope of the distance optic, and thus the global wavefront error map ('near focused, base + lenslets' panel) in *Figure 8* is retained in both the distance and near optic sub-apertures.

4. Discussion

Traditional dual-focus or bifocal lenses designed to be worn by presbyopic and pseudophakic eyes must be able to generate high-quality images at both the distance- and near-

optic focal planes. However, because of the poor image quality generated by the multiple separate PSFs associated with each lenslet of the DIMS lens design at the near add power focal plane (*Figures 4b and 5b*), the extra plus power of the lenslets cannot be used to focus near targets. Since dual-focus optics are now being used to successfully control myopic eye growth in children[7,12] who have large amounts of accommodation[27-29] which can be used to focus near targets, high image quality at the add focal plane is unnecessary. The MTF analysis reveals that the DIMS lens design can generate higher contrast images at low spatial frequencies compared to the traditional bifocal design (*Figure 6*), but because of the fragmented aperture of the distance optic, diffraction limits its ability to generate high contrast high spatial frequency images (*Figures 6 and 7*).

Earlier attempts to control myopic eye growth in children with spectacle lenses were generally unsuccessful.[30,31] However, a study of the DIMS lens by its inventors,[12] revealed a 40% slowing of myopia progression over two years. An ideal myopia control lens should not only control the rate of progression of myopia, but also provide high quality visual performance when looking through the distance optic. Our comparative analysis of the MTF's generated by the DIMS and a zonal bifocal design (Figure *6*) reveal higher contrast generated by the DIMS design, but better spatial detail imaged by the concentric zonal design. The main advantage of the DIMS lens, therefore, other than it being a spectacle design, is that the image demodulation generated by the array of multiple 1 mm diameter lenslets (Figures *4-8*) will be absent for a child viewing through the 10 mm central region of the spectacle lens, which lacks the lenslets. The image demodulation introduced by the multiple lenslets in the DIMS design (Figure *6*) will, therefore, likely be manifest primarily in the peripheral retina. Recent studies in monkeys have shown that the optical characteristics of the peripheral retinal image can control myopic eye growth.[32] The optical results of the DIMS lens in the present study align with this myopia control theory, with the lens providing clear central vision while inducing optical defocus peripherally. Other spectacle lenses designed for myopia control also restrict the image manipulation to the lens periphery[33] as do zonal dual-focus contact lenses where the central zone (e.g. approximately 3.3 mm in the MiSight lens, see Figure *6*) is surrounded by an annular add zone, which contributes significantly to peripheral image generation.[34,35]

Conflict of interest

The authors report no conflicts of interest and have no proprietary interest in any of the materials mentioned in this article.

Author contributions

Mateusz Jaskulski: Data curation-Lead, Formal analysis-Equal, Software-Lead, Visualization-Lead, Writing-review & editing-Equal. **Neeraj Kumar Singh:** Data curation-Equal, Investigation-Equal, Methodology-Equal, Validation-Equal, Writing-original draft-Equal. **Arthur Bradley:** Conceptualization-Equal, Formal analysis-Equal, Investigation-Equal, Methodology-Lead, Project administration-Lead, Software-Equal, Writing-original draft-Lead, Writing-review & editing-Equal. **P Kollbaum:** Conceptualization-Equal, Funding acquisition-Equal, Investigation-Lead, Methodology-Lead, Project administration-Lead, Resources-Equal, Software-Equal, Writing-review & editing-Equal.

References

1. Holden BA, Fricke TR, Wilson DA *et al.* Global prevalence of myopia and high myopia and temporal trends from 2000 through 2050. *Ophthalmology* 2016; 123: 1036–1042.
2. Sun J, Zhou J, Zhao P *et al.* High prevalence of myopia and high myopia in 5060 Chinese university students in shanghai. *Invest Ophth Vis Sci* 2012; 53: 7504–7509.
3. Jung SK, Lee JH, Kakizaki H & Jee D. Prevalence of myopia and its association with body stature and educational level in 19-year-old male conscripts in Seoul, South Korea. *Invest Ophth Vis Sci* 2012; 53: 5579–5583.
4. Flitcroft DI. The complex interactions of retinal, optical and environmental factors in myopia aetiology. *Prog Retin Eye Res* 2012; 31: 622–660.
5. Wu PC, Chen CT, Lin KK *et al.* Myopia prevention and outdoor light intensity in a school-based cluster randomized trial. *Ophthalmology* 2018; 125: 1239–1250.
6. Chia A, Chua WH, Cheung YB *et al.* Atropine for the treatment of childhood myopia: Safety and efficacy of 0.5%, 0.1%, and 0.01% doses (Atropine for the treatment of myopia 2). *Ophthalmology* 2012; 119: 347–354.
7. Chamberlain P, Peixoto de Matos SC, Logan NS *et al.* A 3-year randomized clinical trial of MiSight lenses for myopia control. *Optometry Vision Sci* 2019; 96: 556–567.
8. VanderVeen DK, Kraker RT, Pineles SL *et al.* Use of orthokeratology for the prevention of myopic progression in children: a report by the American Academy of Ophthalmology. *Ophthalmology* 2019; 126: 623–636.
9. Huang J, Wen D, Wang Q *et al.* Efficacy comparison of 16 interventions for myopia control in children: a network meta-analysis. *Ophthalmology* 2016; 123: 697–708.
10. Neitz J, Kuchenbecker J & Neitz M.*Ophthalmic lenses for treating myopia*. United States patent US 20190033619. 2020 Jan 31.
11. To CH, Lam SY, Hatanaka T & Masuda Y.*Spectacle lens.* United States patent US 10,268,050, 2019 Apr 23.
12. Lam CSY, Tang WC, Tse DY *et al.* Defocus Incorporated Multiple Segments (DIMS) spectacle lenses slow myopia

progression: a 2-year randomised clinical trial. *Br J Ophthalmol* 2020; 104: 363–368.
13. Charman WN & Walsh G. Retinal image quality with different designs of bifocal contact lens. *J Br Contact Lens Assoc* 1986; 9: 13–19.
14. Bradley A, Nam J, Xu R, Harman L & Thibos L. Impact of contact lens zone geometry and ocular optics on bifocal retinal image quality. *Ophthal Physl Opt* 2014; 34: 331–345.
15. Davison JA & Simpson MJ. History and development of the apodized diffractive intraocular lens. *J Cataract Refr Surg* 2006; 32: 849–858.
16. Ravikumar S, Bradley A & Thibos LN. Chromatic aberration and polychromatic image quality with diffractive multifocal intraocular lenses. *J Cataract Refr Surg* 2014; 40: 1192–1204.
17. de Gracia P, Dorronsoro C & Marcos S. Multiple zone multifocal phase designs. *Opt Lett* 2013; 38: 3526–3529.
18. Legras R & Rio D. Effect of number of zones on subjective vision in concentric bifocal optics. *Optometry Vision Sci* 2015; 92: 1056–1062.
19. Kollbaum P, Jansen M, Thibos L & Bradley A. Validation of an off-eye contact lens Shack-Hartmann Wavefront Aberrometer. *Optometry Vision Sci* 2008; 85: E817–828.
20. Southwell WH. Wave-front estimation from wave-front slope measurements. *J Opt Soc Am* 1980; 70: 998–1006.
21. Xu R, Bradley A, Lopez Gil N & Thibos LN. Modelling the effects of secondary spherical aberration on refractive error, image quality and depth of focus. *Ophthal Physl Opt* 2015; 35: 28–38.
22. Thibos LN. Calculation of the geometrical point-spread function from wavefront aberrations. *Ophthal Physl Opt* 2019; 39: 232–244.
23. Legras R, Chateau N & Charman WN. A method for simulation of foveal vision during wear of corrective lenses. *Optometry Vision Sci* 2004; 81: 729–738.
24. Ravikumar S, Thibos LN & Bradley A. Calculation of retinal image quality for polychromatic light. *J Opt Soc Am A* 2008; 25: 2395–2407.
25. Kollbaum PS, Jansen ME, Tan J, Meyer DM & Rickert ME. Vision performance with a contact lens designed to slow myopia progression. *Optometry Vision Sci* 2013; 90: 205–214.
26. Smith G. Ocular defocus, spurious resolution and contrast reversal. *Ophthal Physl Opt* 1982; 2: 5–23.
27. Duane A. Normal values of the accommodation at all ages. *J Am Med Assoc* 1912; 59: 1010–1013.
28. Anderson HA, Hentz G, Glasser A, Stuebing KK & Manny RE. Minus-lens-stimulated accommodative amplitude decreases sigmoidally with age: a study of objectively measured accommodative amplitudes from age 3. *Invest Ophth Vis Sci* 2008; 49: 2919–2926.
29. Anderson HA, Glasser A, Manny RE & Stuebing KK. Age-related changes in accommodative dynamics from preschool to adulthood. *Invest Ophth Vis Sci* 2010; 51: 614–622.
30. Walline JJ. Myopia control: a review. *Eye Contact Lens* 2016; 42: 3–8.
31. Sankaridurg P, Donovan L, Varnas S *et al*. Spectacle lenses designed to reduce progression of myopia: 12-month results. *Optometry Vision Sci* 2010; 87: 631–641.
32. Smith EL 3rd. Prentice award lecture 2010: a case for peripheral optical treatment strategies for myopia. *Optometry Vision Sci* 2011; 88: 1029–1044.
33. Neitz J & Neitz M.*Method and apparatus for limiting growth of eye length*. United States patent US16/385810. 2019 Oct 03.
34. Ji Q, Yoo YS, Alam H & Yoon G. Through-focus optical characteristics of monofocal and bifocal soft contact lenses across the peripheral visual field. *Ophthal Physl Opt* 2018; 38: 326–336.
35. Altoaimi BH, Almutairi MS, Kollbaum PS & Bradley A. Accommodative behavior of young eyes wearing multifocal contact lenses. *Optometry Vision Sci* 2018; 95: 416–427.